



## Preparation and physicochemical properties of niclosamide anhydrate and two monohydrates

Elsa C. van Tonder<sup>a</sup>, Tshoane S.P. Maleka<sup>b</sup>, Wilna Liebenberg<sup>a</sup>,  
Mingna Song<sup>d</sup>, Dale Eric Wurster<sup>c</sup>, Melgardt M. de Villiers<sup>d,\*</sup>

<sup>a</sup> *Research Institute for Industrial Pharmacy, Potchefstroom University for Christian Higher Education, Potchefstroom 2520, South Africa*

<sup>b</sup> *Medicines Control Council, Private Bag X828, Pretoria 0001, South Africa*

<sup>c</sup> *College of Pharmacy, The University of Iowa, Iowa City, IA 52242, USA*

<sup>d</sup> *Department of Basic Pharmaceutical Sciences, School of Pharmacy, The University of Louisiana, Monroe, LA 71209, USA*

Received 16 July 2003; received in revised form 23 September 2003; accepted 23 September 2003

### Abstract

The intent of the study was to prepare and characterize three crystal forms of niclosamide namely the anhydrate and the two monohydrates and to investigate the moisture adsorption and desorption behavior of these crystal forms. The crystal forms were prepared by recrystallization and were characterized by differential scanning calorimetry, thermogravimetric analysis, isoperibol solution calorimetry, Karl Fischer titration, and X-ray powder diffractometry. Moisture adsorption by the anhydrate at increased relative humidities and two temperatures, 30 and 40 °C, was measured while the desorption from the monohydrates was determined at 45, 55, and 65 °C for monohydrate H<sub>A</sub> and 75, 90, and 100 °C for monohydrate H<sub>B</sub>. Thermal analysis and solution calorimetry showed that monohydrate H<sub>B</sub> is more stable than monohydrate H<sub>A</sub> and solubility measurements showed the solubility of the crystal forms decreased in the order: anhydrate ≫ monohydrate H<sub>A</sub> > monohydrate H<sub>B</sub>. With an increase in temperature and relative humidity niclosamide anhydrate adsorbed moisture to form monohydrate H<sub>A</sub> by a random nucleation process. Dehydration of monohydrate H<sub>A</sub> at increased temperatures followed zero order kinetics and resulted in a change to the anhydrate. Monohydrate H<sub>B</sub> was transformed to the anhydrate at higher temperatures by a three-dimensional diffusion mechanism.

© 2003 Elsevier B.V. All rights reserved.

**Keywords:** Niclosamide; Hydrates; Solubility; Moisture adsorption; Transformation; Stability

### 1. Introduction

Niclosamide (5-chloro-*N*-(2-chloro-4-nitrophenyl)-2-hydroxybenzamide or 2',5-dichloro-4'-nitrosalicylanilide) (Fig. 1), is used for the treatment of worm infestations in humans and animals such as ruminants, cats, dogs, ostriches and poultry (Reynolds, 1993). It is practically insoluble in water, sparingly

soluble in various other solvents (Merck Index, 2001) and is usually formulated as a suspension, which allows for the development of a liquid dosage form containing an appropriate quantity of drug in a reasonably small volume. Both niclosamide anhydrate and monohydrate are available for formulation (BP, 1993). However, niclosamide anhydrate has a high affinity for water and various suspension formulations form cement-like sediments during storage (Van Tonder, 1996; Caira et al., 1998; Maleka, 2000). With time these sediments become increasingly difficult to disperse (Van Tonder et al., 1998).

\* Corresponding author. Tel.: +1-1318-342-1727;

fax: +1-1318-342-1737.

E-mail address: [devilliers@ulm.edu](mailto:devilliers@ulm.edu) (M.M. de Villiers).

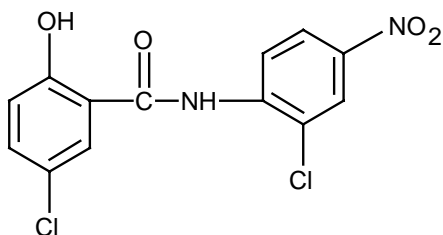


Fig. 1. The chemical structure of niclosamide (MW = 327.1).

Hydration of niclosamide crystals can also be detrimental to the performance of niclosamide powder during various pharmaceutical processes because this drug can be exposed, potentially, to water during crystallization, wet granulation, lyophilization, spray drying, and aqueous film coating. Water can also be taken up during storage in an environment containing water vapor or from excipients that contain water and are capable of transferring it to other ingredients (Khankhari and Grant, 1995). When these niclosamide hydrates are formed, water is incorporated into the crystal lattice.

In general, the water in hydrates is immobilized because it can be: (i) incorporated into the crystalline structure, (ii) linked by hydrogen bonding, or (iii) adsorbed or entrapped within spaces within the structure. In spite of this varying degree of binding, immobile water is generally perceived as not readily available for chemical interaction with other species (Heidemann and Jarosz, 1991). However, it can change the solubility, dissolution and chemical stability of the drug compound. Hydration or solvation is sometimes confused with polymorphism. Polymorphism simply means the existence of the same chemical compound in more than one crystal structure while hydrates are molecular adducts (Wells and Aulton, 1988). Certain hydrates can exhibit polymorphism, e.g., succinyl sulfathiazole monohydrate (Burger and Griesser, 1991). Thus, for a hydrated compound to exhibit polymorphism, the crystal forms should have the same stoichiometry (Khankhari and Grant, 1995).

Since the incorporation of water molecules into the crystal lattice of niclosamide produces compounds with different physical properties, this study was undertaken to determine the conditions under which hydrates are formed and the changes in physicochemical properties brought about by hydration.

## 2. Materials and methods

### 2.1. Materials

Niclosamide (Sigma Chemical Company, St. Louis, USA) and the following analytical grade solvents obtained from Saarchem (Krugersdorp, South Africa) were used, namely acetone, benzene, diethyl ether, dimethyl sulfoxide, *N,N'*-dimethylformamide, ethyl acetate, isopropanol and tetrahydrofuran. Acetonitrile and methanol (BDH, Poole, England), and ethanol (Merck, Darmstadt, Germany) were also used.

### 2.2. Preparation of niclosamide crystal forms

Generally niclosamide raw materials were found to be the anhydrate but this form was also prepared by crystallization from absolute (water free) ethanol, ethyl acetate, benzene and acetone using the following concentrations: ethanol (5% m/v, 3% m/v, 1.5% m/v and 1% m/v); ethyl acetate (2% m/v, 3% m/v); benzene (0.3% m/v); and acetone (3% m/v).

Monohydrate  $H_A$  was obtained by heating a suspension of the anhydrous material in water to boiling point under constant stirring. The suspension was allowed to cool to room temperature and the suspended material was collected by filtration through sintered glass Buchner funnels. The powder was allowed to dry by evaporation at room temperature. Monohydrate  $H_A$  raw materials were also obtained from Bayer (Midrand, South Africa) and Centrachem (Pretoria, South Africa). It was decided to name this monohydrate,  $H_A$ , because it is commercially available. The anhydrate crystallized from a 3% m/v solution in acetone also transformed into  $H_A$  within 8 days when stored at room temperature. Monohydrate  $H_A$  was also crystallized from various concentrations of niclosamide in 95% isopropanol, acetonitrile or ethanol or a 1.5% m/v solution of the anhydrous material in acetone.

The second monohydrate  $H_B$  was formed through the transformation of the anhydrate into transparent, yellow, needle-like crystals when suspended in the crystallizing solvents (ethanol, ethyl acetate, benzene and acetone) and stored in open containers.  $H_B$  was also formed by slow transformation of monohydrate  $H_A$  when stored while it was suspended in the crystallization solvent in open containers.

### 2.3. Morphology of the anhydrate and monohydrates

A scanning electron microscope (Stereoscan 250, Cambridge Scientific Instruments, Cambridge, UK) was used to obtain photomicrographs of the anhydrate and monohydrates H<sub>A</sub> and H<sub>B</sub>. Samples were mounted on a metal stub with an adhesive and coated under vacuum with carbon (Emscope TB500 sputter-coater) before being coated with a thin gold–palladium film (Eiko Engineering Ion Coater IB-2).

### 2.4. Thermal methods of analysis

A Leitz (Laborlux K, Germany) hot-stage microscope was used to visually identify crystals of the different forms. Samples were placed on an object glass, covered with a cover slip and heated to 240 °C at a heating rate of 10 °C/min. Dehydration and desolvation were determined using silicone oil.

DSC traces were recorded with a Shimadzu DSC-50 instrument (Shimadzu, Kyoto, Japan) or a DSC-2920 modulated DSC (TA Instruments, New Castle, DE). Indium (melting point 156.6 °C) and tin (melting point 231.9 °C) were used to calibrate the instruments. A mass, not exceeding 3.0 mg, was measured into aluminum pans with or without a small pin-hole in the lid. DSC curves were obtained under a nitrogen purge of 20 ml/min at a heating rate of 10 °C/min. Heating rates of 5–20 °C/min were used to examine changes in melting points and dehydration peaks.

In those instances where loss of solvent from the crystals was observed in the DSC curves, TGA traces were obtained with either a Shimadzu TGA-50 (Shimadzu) or Hi-Res Modulated TGA-2950 (TA Instruments). TGA traces were recorded at heating rates of 2–10 °C/min under a nitrogen purge of 50 ml/min. Samples with masses between 1 and 10 mg were analyzed using a platinum pan.

### 2.5. X-ray powder diffraction analysis (XRPD)

The XRPD profiles were obtained at room temperature with a Philips PM9901/00 diffractometer. The measurement conditions were: target, CuK $\alpha$ ; filter, Ni; voltage, 40 kV; current, 20 mA; slit, 0.1 mm; scanning speed, 2°/min. Crystals of the different crystal forms were ground into a fine powder with average particle size of  $\pm 60 \mu\text{m}$ . Care was taken to avoid crys-

tal changes during sample preparation. Approximately 200 mg samples were loaded into aluminum sample holders, taking care not to introduce a preferential orientation of the crystals.

### 2.6. Infrared spectroscopy

IR spectra of powdered samples were recorded on a Nexus 470 spectrophotometer (Nicolet Instrument Corporation, MA) over a range of 4000–400 cm<sup>-1</sup> with the Avatar Diffuse Reflectance smart accessory or the KBr disc technique. For diffuse reflectance analysis, samples weighing approximately 2 mg were mixed with 200 mg of KBr (Merck) by means of an agate mortar and pestle, and placed in sample cups for convenient, fast sampling. For the compressed disk technique 2 mg samples were mixed with 200 mg KBr (Merck) by means of an agate mortar and pestle. Discs were pressed using a Beckman 00-25 press (Beckman, Scotland) at a pressure of  $15 \times 10^3 \text{ kg/cm}^2$ .

### 2.7. Aqueous solubility and intrinsic and powder dissolution measurements

Before measuring the aqueous solubility and powder dissolution the different crystals were sieved using a 88- $\mu\text{m}$  sieve and an amount, enough to ensure supersaturation ( $55 \pm 5 \text{ mg}$ ), was measured into test tubes with screw caps. To each test tube 10 ml distilled water was added and the caps were screwed on tightly. The test tubes were rotated at 70 rpm (Heidolph RZR-2000 rotator) in a thermostatically controlled water bath at 25 °C for 24 h. The concentration of nicosamide in the filtered samples was determined spectrophotometrically at 330 nm. The crystal form of the undissolved powder was determined by XRPD and DSC analysis.

The intrinsic dissolution rates (IDR) of the crystals were determined by the propeller-driven method as described by Singh et al. (1968). Powdered samples were slowly compressed with a force of  $2.3 \times 10^5 \text{ kg/cm}^2$  into 13 mm tablets in a die with a Beckmann (type 00-25) IR-press so that the tablet surface was flush with the die surface. Because it had been observed that monohydrate H<sub>A</sub> is influenced by high force compression DSC and TGA traces were obtained before and after measurements to determine if changes in the crystal form had occurred during compression and dissolution. These tests showed that this compression

force did not cause detectable crystal transformation. The back of the die was sealed and mounted directly in a holder in a water-jacketed beaker containing 400 ml of an isopropanol:water (40:60) dissolution medium. A thermostat was used to maintain the temperature at  $25 \pm 1^\circ\text{C}$  while the medium was stirred at 150 rpm. The amount dissolved with time was determined spectrophotometrically.

Powder dissolution was measured according to the method described by Lötter et al. (1983) using apparatus 2 of the USP (USP 24, 2000) (Erweka DT6R, Germany). The dissolution medium was a 40% isopropanol:water mixture thermostatically controlled at  $37 \pm 1^\circ\text{C}$  and stirred at 100 rpm. Fifty milligrams of the powdered crystals were mixed with 25 mg glass beads (0.1–0.11 mm) and vortexed for 1 min in 2 ml of dissolution medium. This was introduced into the 900 ml dissolution medium. The amount of dissolved niclosamide was determined spectrophotometrically. Dissolutions tests were carried out in triplicate.

### 2.8. Determining the activation energy for desolvation from TGA data

The TGA runs for the two monohydrates were obtained at five different heating rates namely, 2, 4, 6, 8, and  $10^\circ\text{C}/\text{min}$ . The negative logarithm of the heating rates was plotted against the inverse of absolute temperature at constant predetermined weight losses. The slopes of the curves were calculated and substituted into the equation,  $E \cong -4.35 \sum \log \beta / \sum (1/T)$ , to obtain the activation energy for the desolvation of the two monohydrates.  $\beta$  is the heating rate ( $^\circ\text{C}/\text{s}$ ) and  $T$  is the absolute temperature (K).

### 2.9. Determining the heats of solution by isoperibol solution calorimetry

Solution calorimetric measurements were performed using a Tronac Model 450 Isoperibol Calorimeter (Tronac, Denver, USA). Data collection and data analysis were facilitated by use of the BASIC language program CALERB and ANAERB (Guillory and Erb, 1985). The solvent employed for analysis consisted of 50 g of 90% w/w *N,N'*-dimethylformamide:water and measurements were performed at  $25^\circ\text{C}$ . The size of samples used in the analysis

ranged from 20 to 40 mg and were weighed (Sartorius Model 1712, MPS) into cylindrical ampoules, the top and bottom faces of which consisted of 12 mm microscope cover slips. The ampoule was submerged into the weighed solvent contained in a Dewar flask, which served as the reaction vessel. The vessel was clamped into position and lowered into the constant temperature water bath maintained at  $25^\circ\text{C}$  with a deviation of  $\pm 0.0004^\circ\text{C}$ . A stirring rate of 400 rpm was employed. An operational heat-capacity calibration to determine the energy equivalent of the system was performed when the reaction vessel temperature reached the set point. Calibration was performed by operating a heater of known resistance ( $101.1\ \Omega$ ) for a carefully measured period of time. Once the heat-capacity calibration was completed, the actual analysis was initiated by mechanically breaking the glass cover slides of the ampoule, and measuring the heat produced when the sample dissolved. In this study, no correction for the heat of mixing of water in the *N,N'*-dimethylformamide:water mixture was made for the enthalpy of hydration, since no significant reaction heat between water and the solvent was involved when mixed.

### 2.10. Gravimetric determination of moisture adsorption and desorption

To measure the moisture uptake of the anhydrate, saturated solutions of the following salts,  $\text{KNO}_3$ ,  $\text{KBr}$ ,  $\text{NaNO}_3$ , and  $\text{MgNO}_3$  were prepared using the method described by Nyqvist (1983). These solutions were used to fill the bottoms of desiccators wherein duplicate samples of  $\pm 100\ \text{mg}$  niclosamide anhydrate contained in small plastic weighing boats were stored. The experiment was carried out at 30 and  $40^\circ\text{C}$  for a period of 28 days. Samples were weighed at appropriate intervals with the aid of Sartorius BP 211D balance and analyzed by both DSC and TGA. For dehydration studies, approximately 100 mg of niclosamide hydrate was accurately weighed into each of ten 2.5 cm diameter glass vials. These samples were put in a vacuum oven at controlled temperatures of 47, 55, and  $65^\circ\text{C}$  ( $\pm 2^\circ\text{C}$ ) for monohydrate  $\text{H}_\text{A}$  and 75, 90, and  $100^\circ\text{C}$  for monohydrate  $\text{H}_\text{B}$ . The samples were removed periodically and weighed on a Sartorius BP 211D balance until a constant weight was reached.

### 2.11. Karl Fischer titration (KFT) water determination

A Metrohm 831 Karl Fischer Automatic Coulometer (Metrohm, Switzerland) was used to determine trace amounts of water in the powdered samples. Results are the mean moisture contents of 5 to 10 different amounts of the samples weighed to the nearest 0.1 mg with a validated balance.

## 3. Results and discussion

In this study, a niclosamide anhydrate and two niclosamide monohydrates, named  $H_A$  and  $H_B$ , were recrystallized from a variety of solvents containing different concentrations of the anhydrate raw material. DSC, TGA, IR, and XRPD analysis and pharmaceutically important solid-state properties including solubility, dissolution, and crystal transformation were used to characterize the crystals so obtained.

### 3.1. Morphology of the crystal forms

SEM photomicrographs of the different crystal forms are shown in Fig. 2. Commercially available raw material was identified as the anhydrate. Crystals of the anhydrate consist of small rectangles and squares. Niclosamide anhydrate is hygroscopic and sorbs moisture, forming needles. Fig. 2(A) shows the needles protruding from the anhydrous material. This photomicrograph was taken of raw material of which the DSC trace showed no dehydration endotherm. A small amount of moisture was already sorbed as can be seen by the formation of needles and the rounded edges of the remaining material. Fig. 2(B) shows a further stage in the hydration process with more needles and less anhydrous phase. The small round needles are built up from smaller round needles. Crystals of monohydrate  $H_A$  can be seen in Fig. 2(C). The crystals consist of rectangular needles with tapered ends. Fig. 2(D) shows the angular needles of monohydrate  $H_B$  in a twisted conformation. This twisted conformation was regularly found among powders containing this monohydrate.

### 3.2. IR-spectroscopic characterization of the crystal forms

According to Moffat et al. (1986) principal peaks of niclosamide analyzed in a KBr disc appear at wavenumbers 1572, 1515, 1613, 1285, 1650, and 1218  $\text{cm}^{-1}$ . In IR spectra (KBr disc) of the anhydrate and monohydrates some of the bands were shifted. The major differences between IR spectra of the anhydrate and monohydrates  $H_A$  and  $H_B$  are listed in Table 1. The hydrated forms of niclosamide can be distinguished from the anhydrate because of the addition of new stretching or bending frequencies resulting from hydration. According to Kosheleva and Bekhli (1974) and Kosheleva et al. (1975) niclosamide can exist in *trans* ( $\beta$ -) and *cis* ( $\alpha$ -) forms, referring to two different conformations and intra-molecular hydrogen bonding arrangements. Single crystal X-ray data confirm that the conformation of niclosamide in the monohydrate  $H_B$  is the  $\beta$  form (Caira et al., 1998). IR spectra of the anhydrate and monohydrates obtained in nujol and 1,4-dioxane also confirmed the presence of the  $\beta$  form.

### 3.3. X-ray crystallographic characterization

Each of the prepared crystal forms had a distinct and characteristic XRPD pattern as shown in Fig. 3. Main X-ray diffraction peak angles and relative intensities for the anhydrate and monohydrates  $H_A$  and  $H_B$  are listed in Table 2. In a previous study, reporting the single crystal structures of several niclosamide inclusion compounds, several interesting points that arose from a comparison of the crystal and molecular structures of the niclosamide solvates were investigated (Caira et al., 1998). With regard to the host drug molecule, only one, nearly planar conformation (the ' $\beta$  form'), is observed in four independent cases. This is sound evidence of the stability of this conformation in the solid state. Close parallel stacking of the niclosamide molecules is a common feature in the crystals, as is the donation of the drug hydroxyl group hydrogen atom to a guest acceptor oxygen atom. In monohydrate  $H_B$  cavity-occupation of the water in the structure was found. However, this compound also formed channel and intercalated inclusion compounds (Caira et al., 1998). For monohydrate  $H_B$  strong host-guest hydrogen bonding and, especially, cavity-occupation by wa-

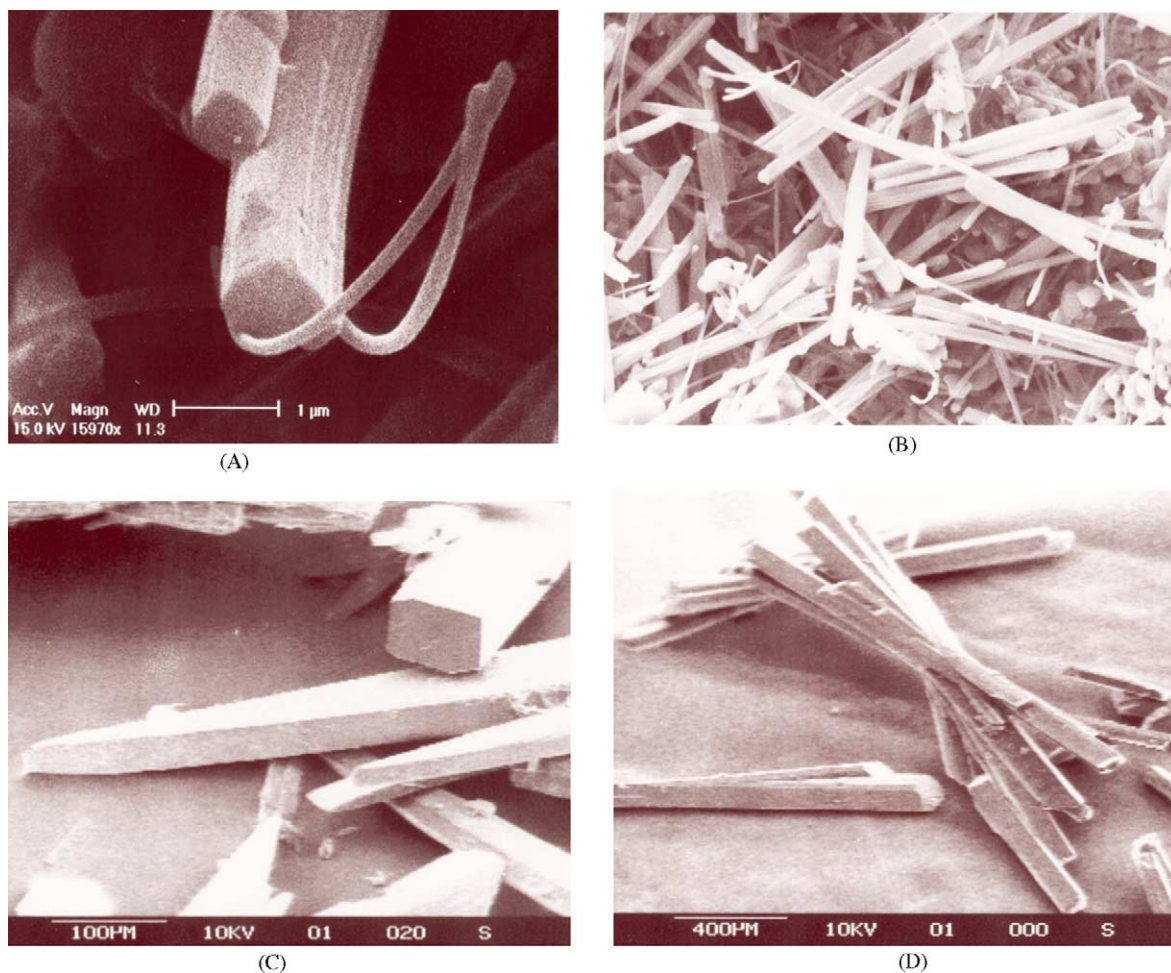


Fig. 2. SEM photomicrographs of niclosamide crystal forms: (A) needles protruding from the crystals of the anhydrous material; (B) anhydrate in a further stage of hydration; (C) monohydrate  $H_A$  crystals; (D) monohydrate  $H_B$  crystals.

Table 1

Wavenumbers, assignments and shifts of the major absorption bands in the IR spectra (KBr disc) of the niclosamide anhydrate and monohydrates

	Wavenumber ( $\text{cm}^{-1}$ ) <sup>a</sup>					
	1613	1650	1572	1285	1515	1218
	Assignment					
	C=C stretch	C=O stretch	N–H bend	C–N stretch	NO <sub>2</sub> stretch	C–O stretch
Anhydrate	1603	1651	1572	1283	1518	1219
Monohydrate $H_A$	Very weak	1680	1570	1289	1507	1223
Monohydrate $H_B$	1611	1655	1555	1281	1505	1221

<sup>a</sup> Moffat et al. (1986).

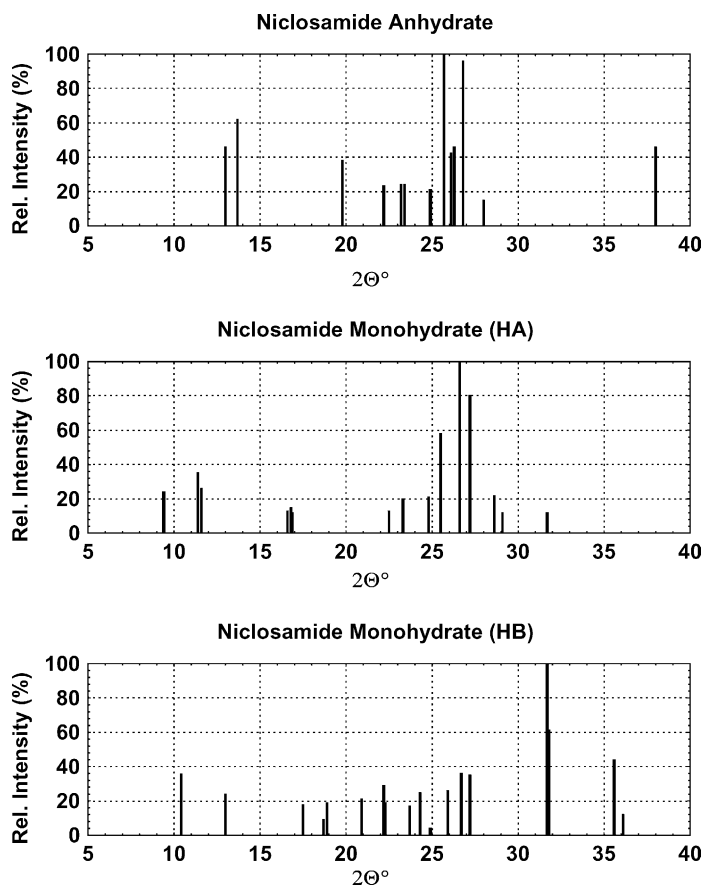
Fig. 3. XRPD patterns of niclosamide anhydrate, monohydrate H<sub>A</sub> and monohydrate H<sub>B</sub>.

Table 2

XRPD  $2\theta$  values,  $d$  spacings and peak heights for the niclosamide anhydrate and monohydrates

Anhydrate			Monohydrate H <sub>A</sub>			Monohydrate H <sub>B</sub>		
$2\theta$ (°)	$d$ (Å)	$I/I_0$ (%)	$2\theta$ (°)	$d$ (Å)	$I/I_0$ (%)	$2\theta$ (°)	$d$ (Å)	$I/I_0$ (%)
25.69	3.466	100.0	26.56	3.353	100.0	27.23	3.273	100.0
26.76	3.329	96.2	27.17	3.279	79.6	31.71	2.820	60.7
13.73	6.444	62.4	25.54	3.485	58.0	31.81	2.811	43.7
12.99	6.807	46.0	11.40	7.756	34.6	25.94	3.433	36.3
26.26	3.389	45.7	9.37	9.436	24.4	26.67	3.340	34.5
38.39	2.343	45.7	28.63	3.115	22.1	20.85	4.257	29.3
26.10	3.411	41.7	24.79	3.589	20.9	24.93	3.570	26.0
19.78	4.485	38.3	23.28	3.819	20.3	23.72	3.748	24.7
23.20	3.832	24.3	37.70	2.384	17.0	10.37	8.528	24.3
23.40	3.799	24.3	16.835	5.262	14.6	18.85	4.704	20.7

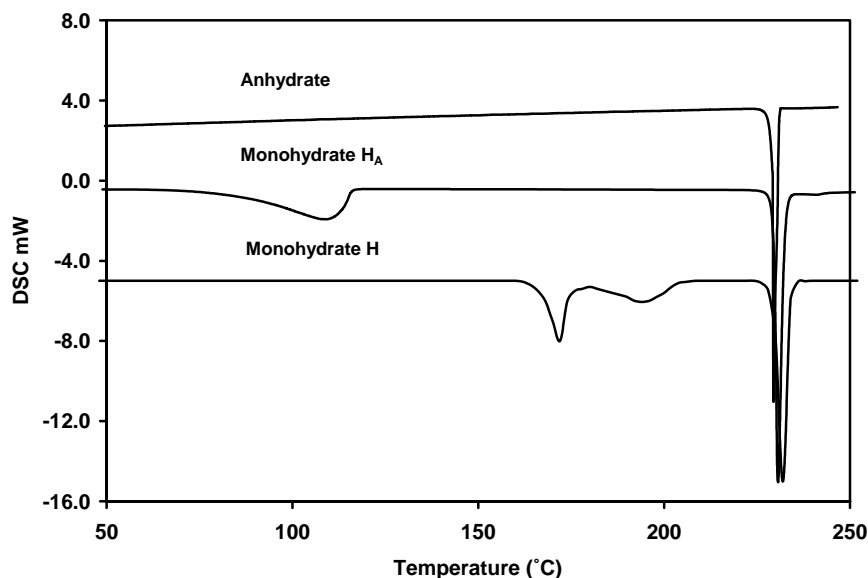


Fig. 4. DSC curves of the niclosamide anhydrate, monohydrates H<sub>A</sub> and monohydrate H<sub>B</sub>.

ter molecules are consistent with the abnormally high peak temperature for dehydration between  $173 \pm 5^\circ\text{C}$  and  $201 \pm 5^\circ\text{C}$ .

### 3.4. Melting points, dehydration temperatures, and enthalpies of melting

DSC traces of the anhydrate and monohydrates are shown in Fig. 4. In Table 3 melting points, dehydration temperatures and enthalpies of melting are listed. The influence of heating rate on the dehydration endotherms of monohydrates H<sub>A</sub> and H<sub>B</sub> is shown in Table 4. Only one endotherm is observed in the DSC trace of the anhydrate. This peak has an onset of  $219 \pm 1^\circ\text{C}$  and a peak maximum at  $229 \pm 0.7^\circ\text{C}$ . The monohydrates dehydrate at different temperatures. H<sub>A</sub>

Table 4

Dehydration endotherms (peak temperatures) and enthalpies for niclosamide monohydrates H<sub>A</sub> and H<sub>B</sub> at different heating rates

Heating rate ( $^\circ\text{C}/\text{min}$ )	Dehydration ( $^\circ\text{C}$ )		Enthalpy (J/g)	
	Peak 1	Peak 2	Peak 1	Peak 2
Monohydrate H <sub>A</sub>				
5	102		90	
10	112		120	
20	125		120	
Monohydrate H <sub>B</sub>				
5	174	199	25	34
10	178	195	62	8
20	184	197	100	5

Table 3

Melting points (peak temperatures), dehydration/desolvation temperatures, weight loss, drug:water stoichiometry and enthalpies for the anhydrate and pseudopolymorphs of niclosamide

Crystal form	Melting point ( $^\circ\text{C}$ )	Enthalpy (J/g)	Dehydration ( $^\circ\text{C}$ )	Enthalpy (J/g)	Range for solvent loss ( $^\circ\text{C}$ )	Mass loss (%)	Drug:H <sub>2</sub> O ratio
Anhydrate	$229 \pm 0.7$	$110 \pm 10$	–	–	–	–	–
Monohydrate H <sub>A</sub>	$228 \pm 0.6$	$110 \pm 10$	$100 \pm 10$	$140 \pm 10$	60–110	$5.02 \pm 0.2$	1:0.96
Monohydrate H <sub>B</sub>	$230 \pm 0.4$	$105 \pm 15$	$173 \pm 5$ $30 \pm 15$	$45 \pm 15$ $201 \pm 5$	170–206	$4.00 \pm 1.3$	1:0.76



dehydrates at  $100 \pm 10$  °C, while  $H_B$  dehydrates in two stages at  $173 \pm 5$  °C and  $201 \pm 5$  °C, respectively. When a DSC trace of  $H_A$  was obtained using a pan with a lid without a pin-hole, the dehydration peak moved to 150 °C which is higher than the temperature required in TGA runs to dehydrate  $H_A$  when open pans were used. Therefore, it was decided to use lids with pin-holes in all of the DSC determinations. An increase in heating rate caused a shift of the dehydration endotherm to higher temperatures for  $H_A$  and the first dehydration peak of  $H_B$  (Table 4). Smaller endotherms with decreased enthalpies of dehydration for  $H_A$  and the first dehydration of  $H_B$  were also seen with an decrease in heating rate. These results are in agreement with the observations made by Giron (1995) who reported that a decrease in the heating rate may lead to total dehydration without detection.

The dehydration behaviors of the monohydrates of niclosamide may also be ascribed to their crystal structures. For example, calcium sulfate dihydrate dehydrates to form a hemihydrate (Giron, 1995). Single crystal X-ray analysis Caira et al. (1998) showed that the water molecules of monohydrate  $H_B$  are very tightly bound inside cavities in the crystals. The water molecules are also extensively involved in hydrogen bonding to host molecules. Dehydration in two differ-

ent DSC-endotherms implies partial loss of water at  $173 \pm 5$  °C and structural rearrangement to yield an intermediate hydrated phase which loses the remaining water at  $201 \pm 5$  °C. In this case, the formation of a definite hemihydrate was not found.

Hot-stage microscopic analysis in silicon oil showed that the crystals of the anhydrate consisted of small rectangles and squares that started melting at 220 °C. The melting was completed at 233 °C. During the heating process, the same events occurred at different temperatures for the monohydrated crystals (Fig. 5). Gas bubbles started to form during dehydration at 90–110 °C for  $H_A$  and 170–200 °C for  $H_B$  (Fig. 5(B)). The crystals start to darken at the lower end of these temperature ranges with a simultaneous slow form change. The form change represents the slow appearance of small rectangle and square crystals forming in the melt (Fig. 5(C)). Some of these rectangles extruded from the needle-like crystals. The rectangles and squares melted at the same temperature as the anhydrate (Fig. 5(D)).

### 3.5. Thermogravimetric measurement of dehydration

Fig. 6 displays the TGA curves of the monohydrates. Theoretically the weight loss from niclosamide

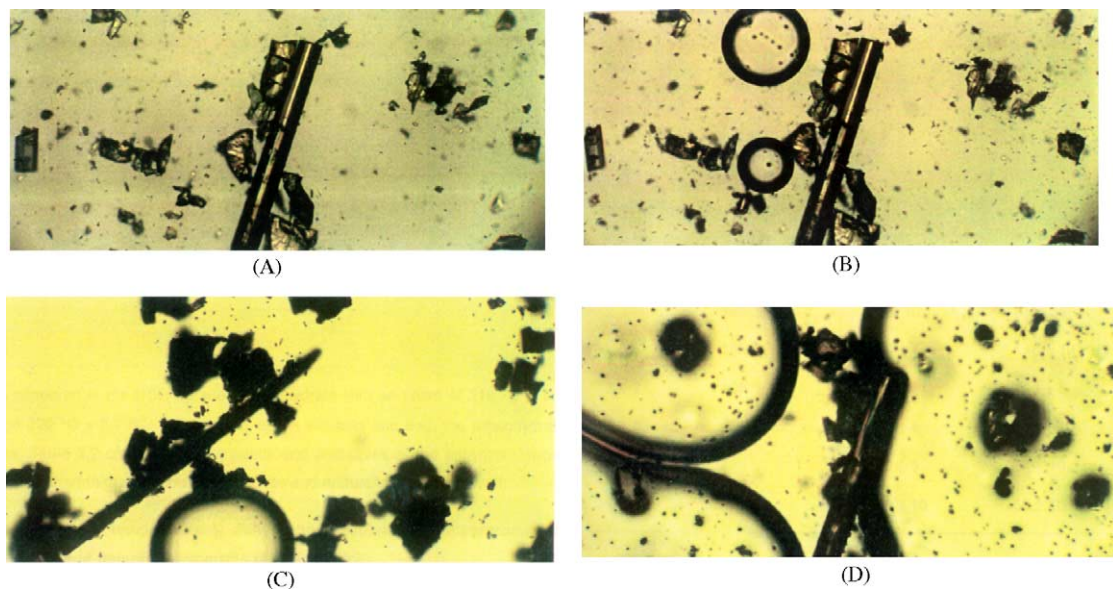


Fig. 5. Photographs of niclosamide monohydrate  $H_B$  at various stages during the heating process in silicone oil: (A) before heating, (B) gas formation, (C) darkened crystals and formed rectangles, (D) melting.

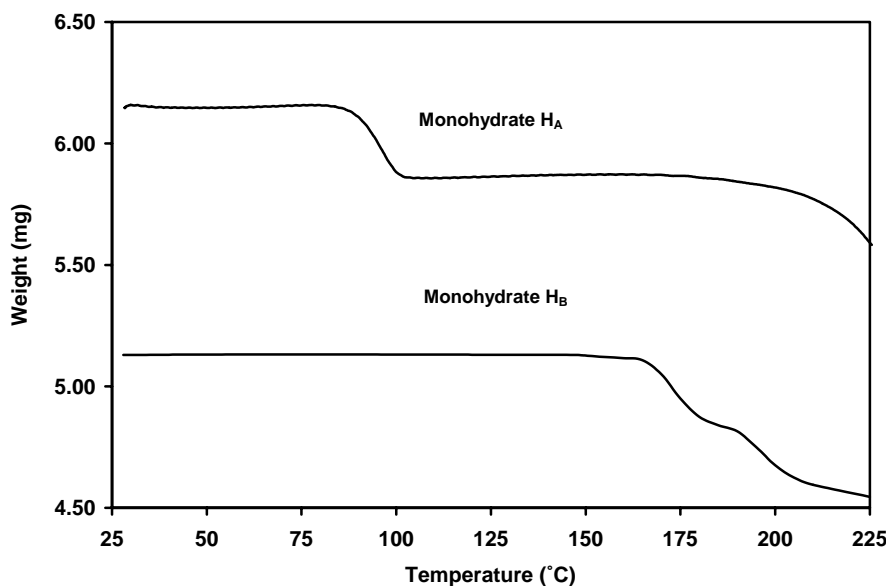


Fig. 6. TGA curves of the niclosamide, monohydrates  $H_A$  and monohydrates  $H_B$ .

monohydrates should be 5.23%. The loss of solvent from the crystals, as well as the stoichiometry of the solvates was determined and results are given in Table 3. These results corresponded with DSC results and the stoichiometric drug:solvent ratios predicted for the crystallization of the two monohydrates,  $H_A$  and  $H_B$ . The moisture contents measured by KFT of the anhydrate and monohydrates  $H_A$  and  $H_B$  were 0.06, 5.01, and 4.93%, respectively. The low moisture content of the anhydrate can be attributed to physically adsorbed moisture and as such this value agrees with TGA results where there was no loss of solvent. The percentage moisture content obtained with KFT for the monohydrates, although slightly lower, was approximately the same as the TGA values.

Thermogravimetric analyses at different heating rates were performed according to the method of

Flynn and Wall (1966) for monohydrates  $H_A$  and  $H_B$ . The negative logarithm of the heating rates is plotted versus the reciprocal of absolute temperature. This plot was used to compute the activation energy necessary for the dehydration of each monohydrate. From the values listed in Table 3, it can be seen that the activation energy for the dehydration of monohydrate  $H_B$  is higher than for monohydrate  $H_A$ . Therefore, monohydrate  $H_B$  is more stable than monohydrate  $H_A$ .

### 3.6. Solubility of the crystal forms

Since different crystal structures are characterized by different lattice energies (and enthalpies) it follows that the solubilities of different crystal polymorphs (or solvated species) must differ as well. In Table 5 the solubilities of the anhydrate and the monohydrates of

Table 5

Solubility in water at 25 °C and IDR in 40% isopropanol:water of niclosamide monohydrates compared to the anhydrate

Crystal form	Solubility of solvated form ( $\mu\text{g/ml}$ )	Solubility equivalent <sup>a</sup> ( $\mu\text{g/ml}$ )	Change to $H_A$ (kJ/mol)	Change to $H_B$ (kJ/mol)	IDR ( $\mu\text{g/cm}^2 \text{ min}$ )
Anhydrate	$13.32 \pm 3.18$	$13.32 \pm 3.18$	-6.69	-7.80	$3.70 \pm 0.03$
Monohydrates $H_A$	$0.95 \pm 0.06$	$0.90 \pm 0.05$	0	-1.15	$3.07 \pm 0.43$
Monohydrates $H_B$	$0.61 \pm 0.09$	$0.58 \pm 0.08$	1.15	0	$2.63 \pm 0.34$

The change in  $\Delta G$  accompanying the conversions also listed.

<sup>a</sup> Solubility converted to equivalent of unsolvated form.

niclosamide in water at 25 °C are listed. The unsolvated equivalent solubilities of the monohydrates were also compared to that of the anhydrate form. The theoretical free energy changes ( $\Delta G$ ) necessary for the spontaneous change of the anhydrate to monohydrate  $H_A$  or  $H_B$  were also calculated using the equation,  $\Delta G (II \rightarrow I) = -RT \ln(S_{II}/S_I)$ , where  $S_{II}$  and  $S_I$  are the solubilities of the anhydrate and monohydrate, respectively (Brittain, 1995). There is a natural tendency for the free energy of a solid system to decrease so that  $\Delta G$  is negative for a spontaneous process. These calculations were done to see if it were theoretically possible for the anhydrate to convert to monohydrate  $H_A$  and  $H_B$ , which was observed from DSC studies of the powders before and after intrinsic dissolution studies. The solubilities of the monohydrate forms (Table 5) were significantly less than that of the anhydrate ( $P < 0.05$ ). Monohydrate  $H_B$  was the least soluble, 0.58  $\mu\text{g/ml}$ . Gibbs free energy values showed that the anhydrate had the highest free energy. The solubility of the crystal forms decreases in the order: anhydrate  $\gg$  monohydrate  $H_A >$  monohydrate  $H_B$  while the stability of the forms estimated from the solubility data are in the reverse order.

### 3.7. Heats of solution of the crystal forms

Since the niclosamide anhydrate and two monohydrates have different solubilities, solution calorimetry was used to measure the heats of solution of these crystal forms. Differences in the heat of solution will be equal to the difference in lattice energy of the solids providing that the solids are chemically identical and differ only in morphology (Lindenbaum and McGraw, 1985). In this study 90% w/w  $N,N'$ -dimethylformamide:water mixtures were used to measure the heats of solution because, although the individual heats of solution will depend on the solvent used, the difference between them is independent of the solvent (Guillory and Erb, 1985). Solution calorimetry is, therefore, a useful technique for obtaining data on the quantitative energy difference between polymorphs or pseudopolymorphs.

First, the heats produced by dissolving different sample weights of the three forms were measured and a plot of heat measured (Joule) versus sample weight (mole) was constructed for each form since, in the case of some compounds in some solvents, association can

Table 6

Heat of solution ( $\overline{\Delta H_s}$ ) and heat of transition ( $\overline{\Delta H_T}$ ) for niclosamide anhydrate and monohydrate

Crystal form	$\overline{\Delta H_s}$ (kJ/mol)	$\Delta H_T \rightarrow H_A$ (kJ/mol)	$\Delta H_T \rightarrow H_B$ (kJ/mol)
Anhydrate	1.10	-5.41	-6.28
Monohydrate $H_A$	6.51	+0.00	-0.86
Monohydrate $H_B$	7.37	+0.86	+0.00

occur between solute molecules at higher concentrations, leading to non-linearity. The mean correlation coefficient obtained by linear regression of the data, was approximately 0.996. This confirmed the fact that, over the range of concentrations studied, there was no measurable change in the extent of interaction occurring between solute molecules. Thus, the individual heat of solution for each crystal form (Table 6) was calculated from the slope of the plot of heat versus sample weight. The intercepts of the plots represent the apparent "enthalpy of ampoule breaking" which was small ( $\approx 0$  J/mol) and reproducible. Partial molar heats of solution and heats of transition summarized in Table 6 indicate that the individual heats of solution were significantly different for the three crystal forms.

For the three forms, the anhydrate has the highest enthalpy (lowest heat of solution) and is the least stable. The transition enthalpy (Table 6) represents an estimate of the difference in thermodynamic stability. A negative value indicates a metastable form converting to a stable form. Therefore, the stability order according to the partial molar heats of solution was monohydrate  $H_B >$  monohydrate  $H_A >$  anhydrate, which is consistent with the stabilities predicted from the solubility data.

### 3.8. Dissolution properties of the crystal forms

In Table 5 the IDR of an anhydrate and monohydrates of niclosamide in a 40% isopropanol:water mixture at 25 °C are listed. Plots of concentration against time were linear. The lines also have intercepts very close to zero (mean y-intercept 0.017 mg). The IDR of monohydrate  $H_A$  was significantly faster than that of monohydrate  $H_B$ , the least soluble crystal form ( $P < 0.05$ ). The dissolution rate of the anhydrate was slightly higher than that of monohydrate  $H_A$ . DSC analyses showed that the anhydrate was quickly transformed to monohydrate  $H_A$  because the dehydration

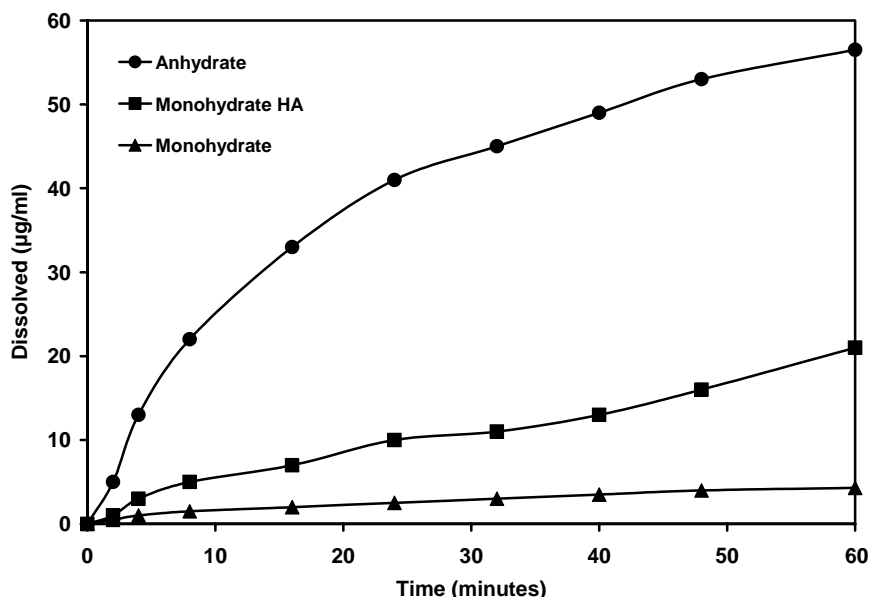


Fig. 7. Powder dissolution curves of niclosamide anhydrate, monohydrates H<sub>A</sub> and monohydrates H<sub>B</sub>.

peak was at 104 °C was observed. This change was also confirmed by XRPD analysis. Although H<sub>A</sub> was not completely changed to H<sub>B</sub> during the time it took to measure the IDR, the results confirmed that the hydrates were the most stable form in water and that H<sub>A</sub> is less stable than H<sub>B</sub>.

Because of the low solubility of niclosamide in water, the dissolution experiments were run in a 40% isopropanol:water mixture. It should be noted that an increase in solubility may increase the tendency for transformation to occur. It has been reported that in the case of chloramphenicol palmitate dissolved in an organic solvent, rapid phase transformation could be observed from form B to form A. Hence, if the transformation of niclosamide polymorphs is solvent-mediated, and the solubility in water is very poor (below 1 mg/ml), then the metastable anhydrate and monohydrate H<sub>A</sub> may have higher bioavailability than the stable form H<sub>B</sub>. However, no further conclusions can be drawn from the available dissolution rate data.

The powder dissolution curves of the different crystal forms are shown in Fig. 7. Although the particle sizes of the powders did not differ significantly, the powder dissolution rates were significantly different and are in accordance with the solubility results. The

anhydrate was again the most soluble and monohydrate H<sub>B</sub> the least soluble. There was also a significant difference between the dissolution rates of the monohydrates.

### 3.9. Differences in moisture sorption and desorption

The results of moisture sorption were analyzed and hydration rates and mechanisms determined based on solid-state kinetic models. To analyze the results, the method employed by Yoshihashi et al. (1998) was followed. DSC and solution calorimetry showed monohydrate H<sub>B</sub> to be more stable than either monohydrate H<sub>A</sub> or the anhydrate. Solubility was in the order: anhydrate  $\gg$  monohydrate H<sub>A</sub> > monohydrate H<sub>B</sub>. However, the solubilities of all the crystal forms were very low in water, all below 1 mg/ml. It should be emphasized that the solubility difference between polymorphs or solvates will be maintained only when the less stable form cannot convert to the most stable form. The question then became how differences in the energy for desolvation and heat of solution correlate with the interconversion of the crystal forms. Thermal analysis results showed that in the presence of water the anhydrate would eventually transform to one of the monohydrates.

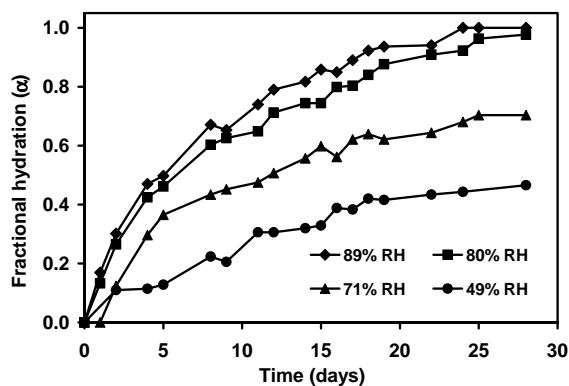


Fig. 8. Powder hydration profiles at 40°C and increasing relative humidity for niclosamide anhydrate.

The mechanism of hydration of niclosamide anhydrate at 30 and 40°C was determined with the aid of the following equation:  $\ln(-\ln(1-\alpha)) = m \ln(t) + \ln(B)$ , where  $\alpha$  is fractional hydration of the anhydrate,  $B$  is a constant and  $m$  is a constant related to an intrinsic value determined from various theoretical equations for the solid-state decomposition (Yoshihashi et al., 1998). Fig. 8 shows the fractional hydration ( $\alpha$ ) of niclosamide anhydrate with time at four different RH's and 40°C. The mechanism of hydration of niclosamide anhydrate was determined by calculating the value of  $m$  from the slope of the plot of  $\ln(-\ln(1-\alpha))$  versus  $\ln(t)$ . Since the calculated  $m$  value of  $0.822 \pm 0.08$  is closest to 1 when rounded to the nearest decimal, it is proposed that the hydration of niclosamide anhydrate follows the mechanism of random nucleation (with one nucleus on each particle). Residual analysis confirmed that the observed linear equation was not simply a chance occurrence but a real relationship between the variables.

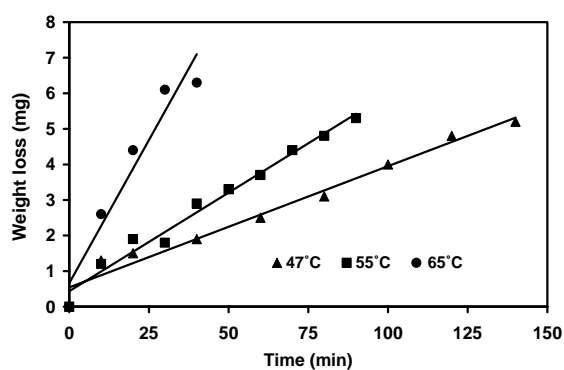


Fig. 9. Dehydration of monohydrate  $H_A$  as measured by the weight loss at 47, 55, and 65°C.

Having determined the mechanism of hydration of niclosamide anhydrate as random nucleation the rate of hydration of niclosamide anhydrate can be calculated using the equation,  $\ln(1-\alpha) = k(t)$ . This equation was used to determine the rates of hydration of niclosamide anhydrate at 30 and 40°C. From the slopes of the plots of  $-\ln(1-\alpha)$  versus time at the two temperatures, the rates ( $k_{\text{obs}}$ ,  $\text{day}^{-1}$ ) of hydration were obtained from the slopes of the curves. The slopes of the plots and their regression coefficients are listed in Table 7. Using the information in Table 7, the rate constant for the hydration of niclosamide anhydrate was calculated from the slopes obtained when plotting  $k_{\text{obs}}$  versus relative humidity at 30 and 40°C. These results, Table 7, showed that the rate constant for the hydration of the anhydrate increases with an increase in temperature. With the aid of these rate constants, the rates of hydration at any relative humidity can be predicted by using the equation  $k_{\text{obs}} = k'(RH)$ , where  $k'$  is the rate constant at a particular temperature and RH is the relative humidity.

Table 7  
Change in the rate of hydration for the anhydrate as a function of relative humidity

Temperature (°C)	Relative humidity (%)	Slope ( $k_{\text{obs}}$ , $\text{day}^{-1}$ )	y-intercept	$R^2$ value	$k'$ ( $\text{day}^{-1}$ )
30	93	0.123	0.376	0.969	0.0041
	80	0.101	0.277	0.937	
	70	0.044	0.142	0.922	
40	89	0.130	0.026	0.982	0.0026
	80	0.101	0.048	0.984	
	71	0.045	0.149	0.954	
	49	0.026	0.036	0.965	

Slopes of the plot of  $-\ln(1-\alpha)$  vs., time the anhydrate at 30 and 40°C.

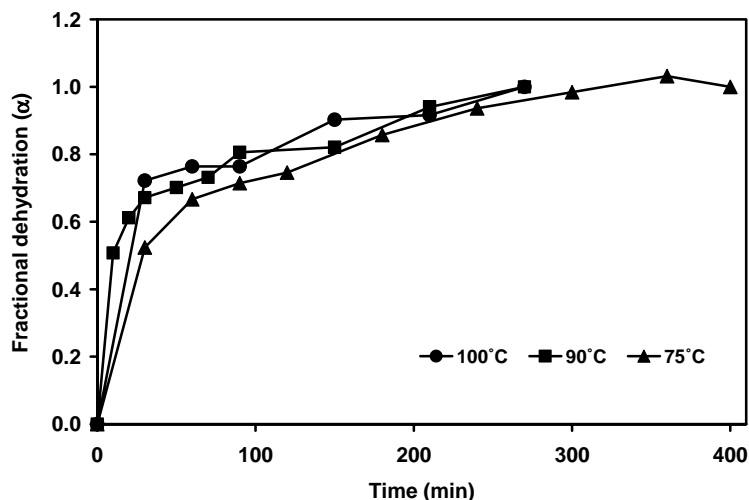


Fig. 10. Powder dehydration profiles at increasing temperatures for monohydrate  $H_B$ .

Fig. 9 shows the dehydration of monohydrate  $H_A$  at 47, 55, and 65 °C. The dehydration of this monohydrate follows the zero order kinetics since there is a linear relationship between mass loss and time. The rate of dehydration  $k_{obs}$  of monohydrate  $H_A$  at each temperature can be obtained from the slope of the plot of mass decrease versus time, and when the logarithm of  $k_{obs}$  is plotted against temperature a linear relationship between the two results ( $R^2 = 0.9783$ ) was seen. The rate constant  $k$ , for the dehydration of monohydrate  $H_A$  obtained from the slope of this plot was 0.0378. Substituting this constant in the equation  $\log k_{obs} = kT$ , the rate of dehydration of monohydrate  $H_A$  at any temperature can be predicted.

For monohydrate  $H_B$  there was no linear relationship between mass decrease and temperature, thus in order to determine the rate and mechanism of dehydration, the method of Yoshihashi et al. (1998) was again employed. Fig. 10 shows the fractional dehydration ( $\alpha$ ) plotted against time at three temperatures, 75, 90, and 100 °C. From the plot it is clear that it took almost the same time for dehydration to be completed for the samples at 90 and 100 °C, while at 75 °C the process took longer.

In determining the mechanism of dehydration of monohydrate  $H_B$  plots of  $\ln(-\ln(1-\alpha))$  versus  $\ln(t)$  were used to obtain  $m$ . Using this method  $m$  was found

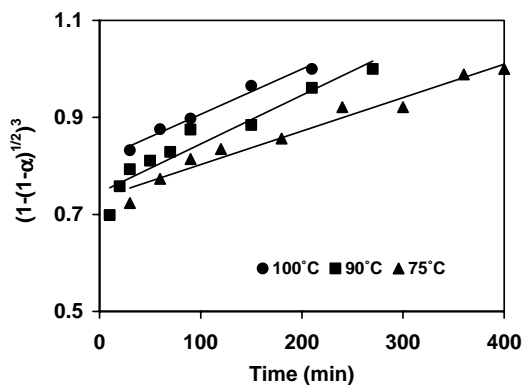


Fig. 11. Plots showing the linear fit for the dehydration of monohydrate  $H_B$  as described by the Jander equation (Yoshihashi et al., 1998).

to be 0.4856 ( $\pm 0.0254$ ) and according to Yoshihashi et al. (1998) this suggests the mechanism of dehydration of monohydrate  $H_B$  was that of three-dimensional diffusion described by the Jander equation,  $(1 - (1 - \alpha)^{1/3})^2 = kt$  as shown in Fig. 11.

#### 4. Conclusion

A niclosamide anhydrate and two monohydrates  $H_A$  and  $H_B$  were prepared by crystallization from sev-

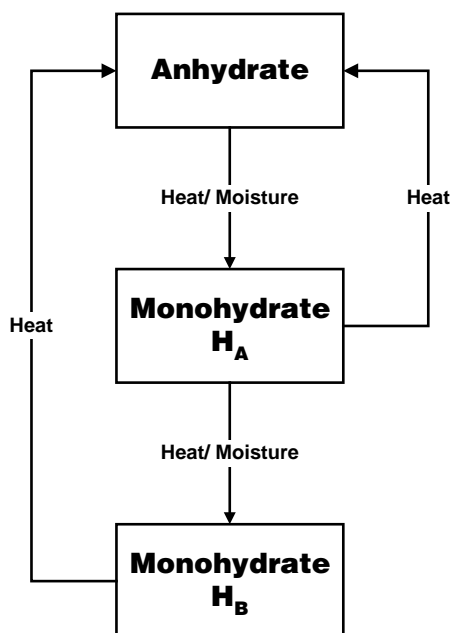


Fig. 12. Stability relationships between the niclosamide crystal forms reported in this study.

eral solvents. These crystal forms were identified and characterized from differences in DSC, TGA, XRPD, solution calorimetry and Karl Fischer titration analysis. It was established that the solubility of the crystal forms in water decreased in the order: anhydrate  $\gg$  monohydrate  $H_A$  > monohydrate  $H_B$ . The activation energy necessary for the desolvation of the two monohydrates was determined and predicted the stability of the crystal forms to be in the order: monohydrate  $H_B \gg$  monohydrate  $H_A$  > anhydrate. Moisture sorption experiments showed that temperature played an important role in the rate and the extent of moisture sorption by the anhydrate. The niclosamide anhydrate sorbs moisture by way of random nucleation with one nucleus on each particle. Dehydration studies on monohydrate  $H_A$  showed it loses crystalline water by zero order kinetics and monohydrate  $H_B$  undergoes loss of water of crystallization through three-dimensional diffusion. Dehydration of the two monohydrates transforms these powders back into the anhydrate. In summary, the stability relationships between the various niclosamide crystal forms, under the conditions reported in this study, are shown in Fig. 12.

## Acknowledgements

This work was supported by grants from the National Research Foundation (Pretoria, South Africa) and the Louisiana Board of Regents Enhancement Program (LEQSF(2001-02)-ENH-TR-82). Research support from the University of Iowa is also acknowledged.

## References

- British Pharmacopoeia, 1993. Her Majesty's Stationary Office, London, p. 445.
- Brittain, H.G., 1995. Physical Characterization of Pharmaceutical Solids. Marcel Dekker, New York, pp. 322–327.
- Burger, A., Griesser, U.J., 1991. The polymorphic drug substances of the European Pharmacopoeia. Part 7. Physical stability, hygroscopicity, and solubility of succinylsulfathiazole crystal forms. *Eur. J. Pharm. Biopharm.* 37, 118–124.
- Caira, M.R., Van Tonder, E.C., De Villiers, M.M., Lötter, A.P., 1998. Diverse modes of solvent inclusion in crystalline pseudopolymorphs of the anthelmintic drug niclosamide. *J. Incl. Phenom. Mol. Rec. Chem.* 31, 1–16.
- Flynn, J.H., Wall, L.A., 1966. Quick, direct method for determination of activation energy from thermogravimetric data. *Pol. Lett.* 4, 323–328.
- Giron, D., 1995. Thermal analysis and calorimetric methods in the characterization of polymorphs and solvates. *Therm. Acta* 248, 1–59.
- Guillory, J.K., Erb, D.M., 1985. Using solution calorimetry to quantitate binary mixtures of the three crystalline forms of sulfamethoxazole. *Pharm. Manufact.*, 2, Sept, 29–33.
- Heidemann, D.R., Jarosz, J., 1991. Preformulation studies involving moisture uptake in solid dosage forms. *Pharm. Res.* 8, 292–297.
- Khankhari, R.K., Grant, D.W., 1995. Pharmaceutical hydrates. *Therm. Acta* 248, 61–79.
- Kosheleva, L.I., Bekhli, A.F., 1974. Polymorphic modifications of phenasal and their IR spectra. *Khimiko-farmatsevticheskii Zhurnal* 8, 57–60.
- Kosheleva, L.I., Shumakovich, I.E., Bekhli, A.F., 1975. IR spectra and structure of substituted salicylanilides. *Zhurnal Obschei Khimii* 45, 407–411.
- Lindenbaum, S., McGraw, S.E., 1985. The identification and characterization of polymorphism in drug solids by solution calorimetry. *Pharm. Manufact.*, 2, Jan, 27–30.
- Lötter, A.P., Flanagan, D.R., Palepu, N.R., Guillory, J.K., 1983. A simple reproducible method for determining dissolution rates of hydrophobic powders. *Pharm. Technol.* 7, 55–66.
- Maleka, T.S.P., 2000. Aqueous adsorption and desorption behaviour of niclosamide anhydrate and monohydrates. M.Sc. Dissertation, Potchefstroom University for CHE, South Africa.
- Merck Index, 13th ed., 2001. Merck, New Jersey, p. 1030.
- Moffat, A.C., Jackson, J.V., Moss, M.S., Widdop, B., 1986. *Clarke's Isolation and Identification of Drugs in Pharmaceuticals, Body Fluids, and Post-mortem Materials*, 2nd ed. Pharmaceutical Press, London.

- Nyqvist, H., 1983. Saturated salt solutions for maintaining specified relative humidities. *Int. J. Pharm. Technol. Prod. Manufact.* 4, 47–48.
- Reynolds, J.G.F., 1993. *Martindale: The Extra Pharmacopeia*, 30th ed. Pharmaceutical Press, London, p. 48.
- Singh, P., Desai, S.J., Flanagan, D.R., Simonelli, A.P., Higuchi, W.I., 1968. Mechanistic study of the influence of micelle solubilization and hydrodynamic factors on the dissolution rate of solid drugs. *J. Pharm. Sci.* 57, 959–965.
- Van Tonder, E.C., 1996. Preparation and characterisation of niclosamide crystal modifications. Ph.D. Thesis, Potchefstroom University for CHE, South Africa.
- Van Tonder, E.C., Lötter, A.P., De Villiers, M.M., Caira, M.R., Liebenberg, W., 1998. Correlation between hydrate formation and the physical instability of suspensions prepared with different niclosamide crystal forms. *Pharm. Ind.* 60, 722–725.
- Wells, J.I., Aulton, M.E., 1988. Preformulation. In: Aulton, M.E. (Ed.), *Pharmaceutics: The Science of Dosage Form Design*. Churchill, New York, pp. 223–253.
- Yoshihashi, Y., Makita, M., Yamamura, S., Fukuoka, E., Terada, K., 1998. Determination of the heat of hydration and hydration kinetics of theophylline by thermal analysis. *Chem. Pharm. Bull.* 46, 1148–1152.